Electronic Supporting Information

Rapid and high-yield production of g-C_3N_4 nanosheets via chemical exfoliation for photocatalytic H_2 evolution†

Jincheng Tong, Li Zhang,* Fei Li, Ke Wang, Lifen Han and Shaokui Cao*

Received (in XXX, XXX) Xth XXXXXXXXX 20XX, Accepted Xth XXXXXXXXX 20XX
DOI: 10.1039/b000000x

S1 Experimental section

Preparation of samples

Preparation of bulk g-C_3N_4: Bulk g-C_3N_4 was prepared by direct pyrolysis of melamine in a semi-closed system. In detail, 10 g of melamine was placed in a 50 mL crucible, then the crucible was wrapped up with aluminium-foil and heated to 550 ^{o}C in a tube furnace for 4 h with a heating rate of 5 ^{o}C/min, and the cooling rate was controlled at around 2 ^{o}C/min. The resultant light yellow agglomerates (6 g) were milled into powders in an agate mortar.

Preparation of g-C_3N_4 nanosheets: The as-prepared g-C_3N_4 (1 g) was mixed with 15mL of concentrated H_2SO_4 (98 wt%) in a 100 mL flask and stirred for 15 min. Then 0.5 mL distilled water was added into the suspension dropwise with stirring, and the temperature of the suspension was rapidly increased to 60 ^{o}C due to the simultaneous exothermic process. 4.5 mL water was then slowly added into the suspension in 10 min to maintain the temperature constant and the color of the suspension turned from light yellow to white. The resulting suspension was poured into 500 mL distilled water, filtered through a 0.22 μm microporous membrane, and washed thoroughly with distilled water to remove the residual acid. The obtained product was redispersed into 200 mL distilled water under the aid of ultrasonication, and then centrifuged at 3000 rpm to remove any unexfoliated g-C_3N_4. The supernatant was collected and concentrated on a rotary evaporator at 60 ^{o}C under reduced pressure, resulting in a dense suspension. Then the suspension was dried at 60 ^{o}C in vacuum overnight. The product yield was measured to be 0.7 g.

Characterizations

Atomic force microscope (AFM) images were acquired in phase mode in air using a Digital Instrument Shimadzu SPM-9500 (samples were prepared by drop-casting corresponding dilute dispersions onto freshly cleaved mica surface). Morphologies of the products were examined by a JEOL JSM-7001F scanning electron microscope (SEM). Transmission electron microscopy (TEM) images were recorded using a JEOL model JEM 2010 EX microscope at an accelerating voltage of 200 kV. Zeta potential was measured using a Malvern Zetasizer Nano ZS90 and the suspensions of each material in aqueous solution media (0.1 mg/mL) were prepared and measured. X-ray diffraction (XRD) patterns were characterized on a PANalytical's X'Pert PRO MRD using Cu irradiation. Fourier transformed infrared (FTIR) spectra were recorded on a Bruker VERTEX 700 spectrometer between 4000 and 400 cm^{-1}. Brunauer–Emmett–Teller (BET) specific surface area was characterized by nitrogen adsorption at 77 K with Micromeritics ASAP 2020 instrument. UV-Vis Diffuse reflection spectra (DRS) were obtained on an Agilent Cary 5000 UV-Vis-NIR spectrophotometer. Photoluminescence spectra (PL) were obtained at room temperature excited by incident light of 380 nm using a PTI QuantaMaster 40 phosphorescence/fluorescence spectrofluorometer. X-ray photoelectron microscopy (XPS) was performed on an ESCALAB 250 photoelectron spectrometer (Thermo Fisher Scientific) with Al Kα (1486.6 eV) as the X-ray source set at 150 W and a pass energy of 30 eV for high-resolution scan.

Photoelectrochemical measurements

Photoelectrochemical measurements were performed on a RST5000 electrochemical workstation (Suzhou Risetest Instrument Co., Ltd) using a conventional three-electrode cell with a Pt sheet and a saturated calomel electrode as the counter electrode and the reference electrode, respectively. The visible light was generated by a 300 W Xe arc lamp with a UV-cutoff filter (λ>400 nm). The electrolyte was a 0.1 M Na_2SO_4 aqueous solution. The working electrodes were prepared as follows: 0.25 mg of the as-prepared photocatalyst was suspended in 0.25 mL of water to produce slurry, which was then dip-coated on a 20 mm×30 mm indium-tin oxide (ITO) glass electrode. After air drying, the electrodes were heated at 180 ^{o}C in air for 3h. Uncoated parts of the ITO electrode were isolated with electrical tape and the exposed area of the working electrode was 2 cm^2. The working electrodes were immersed in the electrolyte for 60 s before any measurement was taken. The photoelectrochemical measurements were conducted with the glass side of working electrode facing the incident light to minimize the influence of thickness of the semiconductor layer. The photocurrent response were measured under a chopped light irritation (chopping frequency: 0.25 Hz) using scanning potential from -0.5 V to 1.0 V with a scan rate of 5 mV s^{-1}. Electrochemical impedance spectroscopy (EIS) was carried out at the open circuit potential. A sinusoidal ac perturbation of 5 mV was applied to the electrode over the frequency range 0.01 to 10^5 Hz.

Photocatalytic activities

Photocatalytic tests were carried out in a quartz top-irradiation vessel under a parallel light source system. A 210 W Xe arc lamp with a UV-cutoff filter ($\lambda>400$ nm) was used as light source for photocatalytic H_2 evolution from water. In a typical test, 20 mg of g-C_3N_4 sample was dispersed into an aqueous solution (100 mL) containing triethanolamine (10 vol. %) as sacrificial electron donor. A co-catalyst of Pt nanoparticles was introduced through *in situ* photodeposition, where 3 wt. % (respect to Pt) $H_2PtCl_6{\cdot}6H_2O$ was added and well distributed in the reaction system. Prior to irradiation, the reaction system was evacuated several times to remove air completely. The evolved gases were analyzed by gas chromatography equipped with a thermal conductive detector (TCD) and a 5Å molecular sieve column, using nitrogen as the carrier gas. Temperature of the reaction solution was maintained at about 20 ^{o}C by cooling water flowing during the reaction.

S2 Additional information of bulk g-C_3N_4 and g-C_3N_4 nanosheets

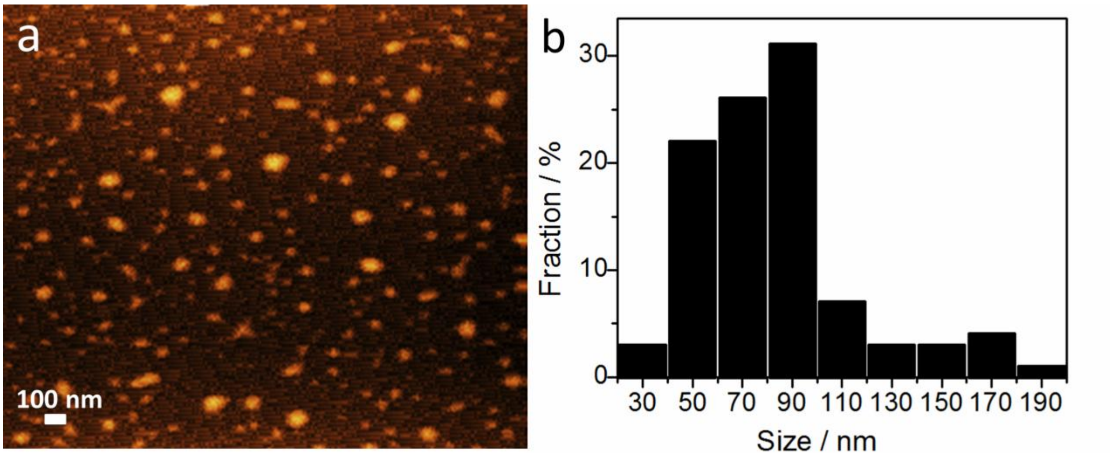

Fig. S1 (a) Enlarged AFM image and (b) the size distribution of as-prepared g-C_3N_4 nanosheets.

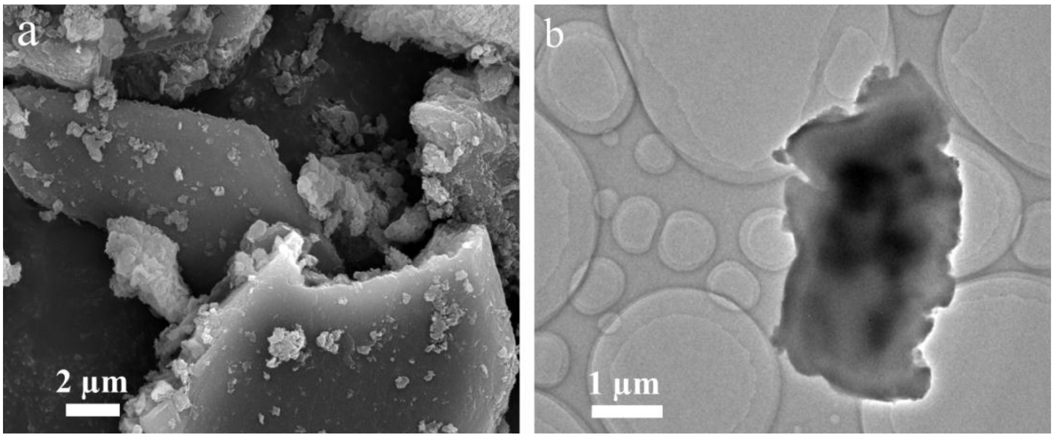

Fig. S2 (a) SEM image and (b) TEM image of bulk g-C_3N_4.

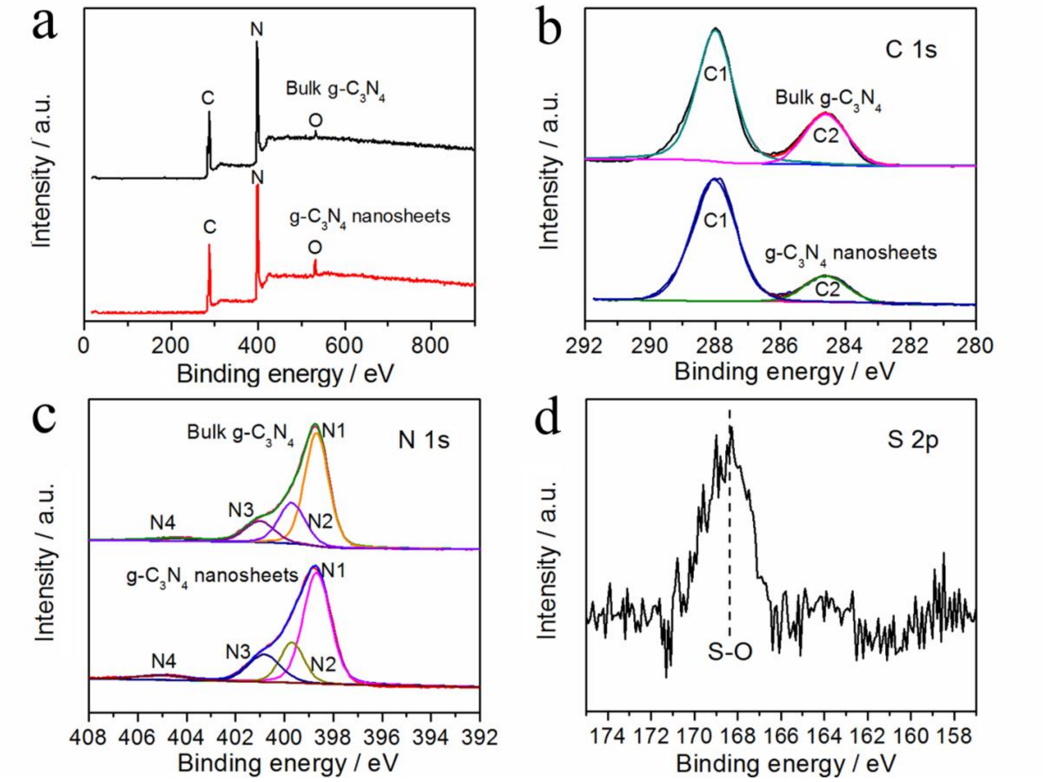

Fig. S3 (a) XPS survey spectra, (b) C 1s XPS spectra and (c) N 1s XPS spectra of bulk g-C_3N_4 and g-C_3N_4 nanosheets. (d) S 2p XPS spectra of g-C_3N_4 nanosheets.

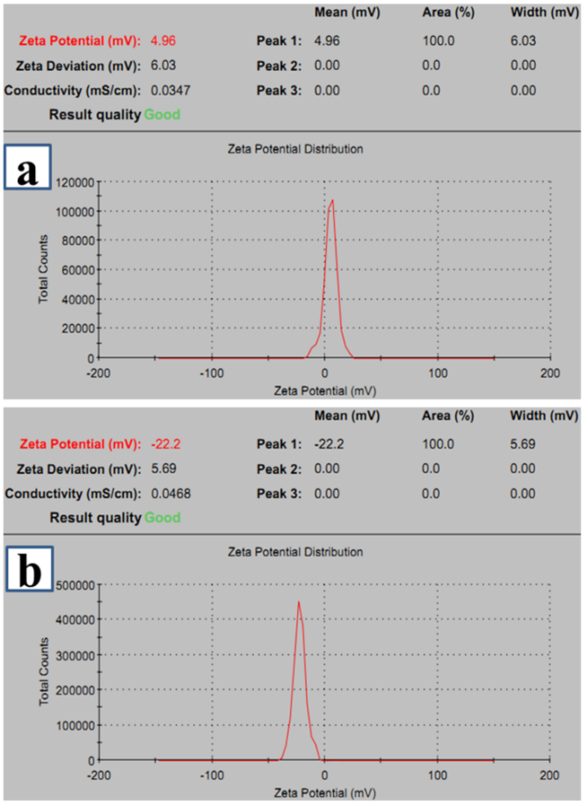
```
                                          Mean (mV)   Area (%)   Width (mV)
  Zeta Potential (mV): 4.96       Peak 1: 4.96        100.0      6.03
  Zeta Deviation (mV): 6.03       Peak 2: 0.00        0.0        0.00
Conductivity (mS/cm): 0.0347      Peak 3: 0.00        0.0        0.00
       Result quality Good
```

```
                                          Mean (mV)   Area (%)   Width (mV)
  Zeta Potential (mV): -22.2      Peak 1: -22.2       100.0      5.69
  Zeta Deviation (mV): 5.69       Peak 2: 0.00        0.0        0.00
Conductivity (mS/cm): 0.0468      Peak 3: 0.00        0.0        0.00
       Result quality Good
```

Fig. S4 Zeta potential of (a) g-C_3N_4 nanosheets and (b) bulk g-C_3N_4 dispersed in water.

S3 Mechanism of the exfoliation process of g-C_3N_4

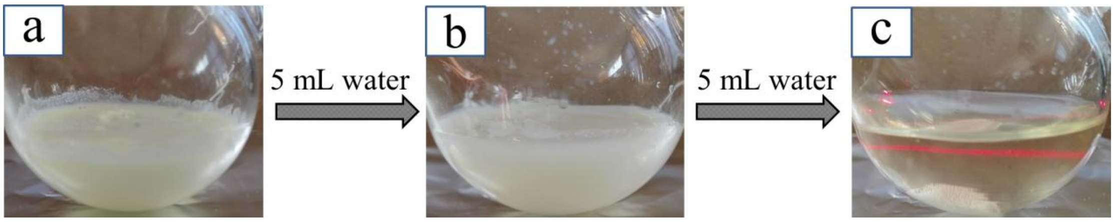

Fig. S5 Photos of (a) the initial suspension consisted of bulk g-C_3N_4 and concentrated H_2SO_4, (b) the suspension after 5 mL H_2O was added, and (c) the suspension after a total amount of 10 mL water was added and its Tyndall effect.

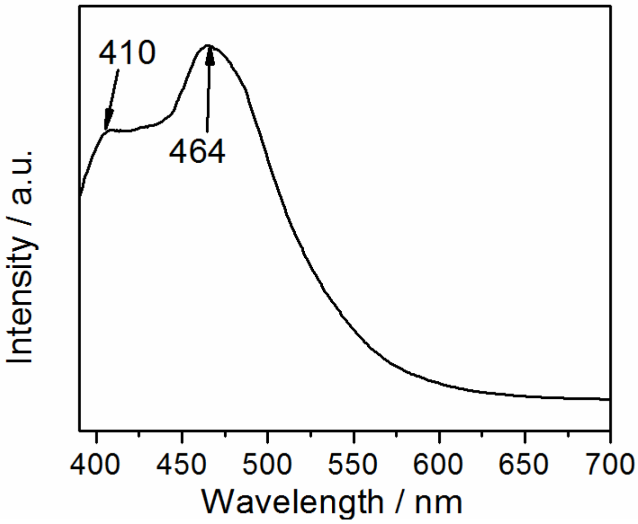

Fig. S6 PL spectra of the transparent suspension in Fig. S5c.

The transparent suspension in Fig. S5c was poured into 50 mL distilled water and the white precipitate was obtained. This precipitate was filtered, washed with distilled water to neutral and dried, and was notated as P1. The collected filtrate from the above filter process was further poured into 200 mL ethanol and the other white precipitate was also obtained. This precipitate was washed with ethanol and water to neutral and dried, and was notated as P2. According to these precipitation process, it is obvious that the precipitate obtained from water (P1) has a lower degree of exfoliation compared to the successive precipitate from ethanol (P2).

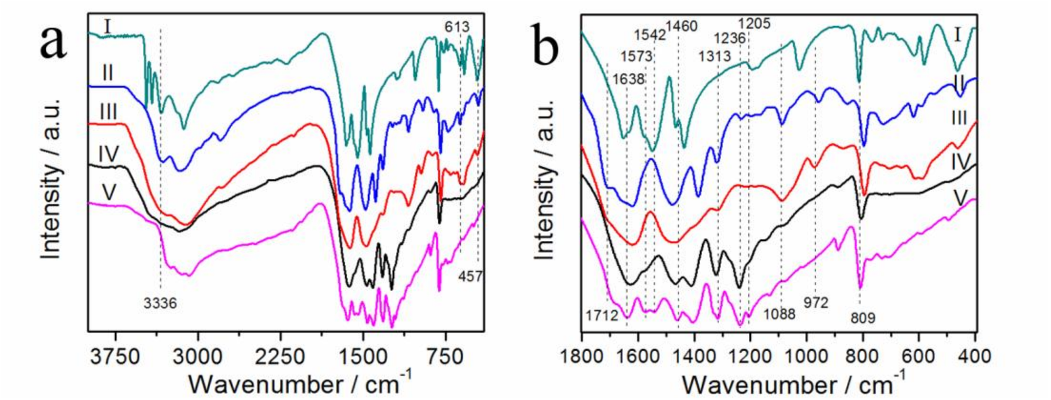

Fig. S7 (a) FTIR spectra of (I) Melamine, (II) P2, (III) P1, (IV) g-C_3N_4 nanosheets and (V) bulk g-C_3N_4. (b) Enlarged FTIR spectra of I, II, III, IV and V from 400 to 1800 cm^{-1} showing more details.

The FTIR spectra of P1 and P2 are shown in Figure S8, together with the spectra of melamine, g-C_3N_4 nanosheets and bulk g-C_3N_4 for comparison. Firstly, the spectra of precipitates are quite different to that of melamine, ruling out the decomposition of g-C_3N_4 into its precursor molecules. Compared with bulk g-C_3N_4, the peaks at 1638 and 809 cm^{-1} shift to lower wavenumber, the peak at 1460 cm^{-1} shifts to higher wavenumber, and the peaks at 1573 cm^{-1} and 1542 cm^{-1} becomes unobvious for g-C_3N_4 nanosheets and precipitates. These five peaks are attributed to the C=N vibrations in the tri-s-triazine ring, which indicates the protonation of triazine conjugated ring during acid treatment.[1] Furthermore, some other band changes can be observed for nanosheets and precipitates, which are associated with the disintegration of bulk g-C_3N_4. The emergence of new peaks at 3336 cm^{-1} (-NH_2 symmetric stretching), 613 cm^{-1} (-NH_2 wag) and 457 cm^{-1} (-NH_2 bend and rock) for nanosheets and precipitates, as well as the blue-shift of N-H signals (3000-3500cm^{-1}) in comparison with bulk g-C_3N_4, suggests the dissociation of hydrogen-bonds in g-C_3N_4 network.[2, 3] Also, the peaks at 1205, 1236 and 1313 cm^{-1}, which corresponds to the bridging C-NH-C units,[4] gradually decreased with adding water, and meanwhile some new peaks located at 1712 cm^{-1} (C=O stretching), 1088 cm^{-1} (C-O stretching) and 972 cm^{-1} (N-O stretching) appear for nanosheets and precipitates,[3, 5] indicating the cleavage of bridging bond -NH- between tri-s-triazine units due to the hydrolysis/oxidation during in the exfoliation process.

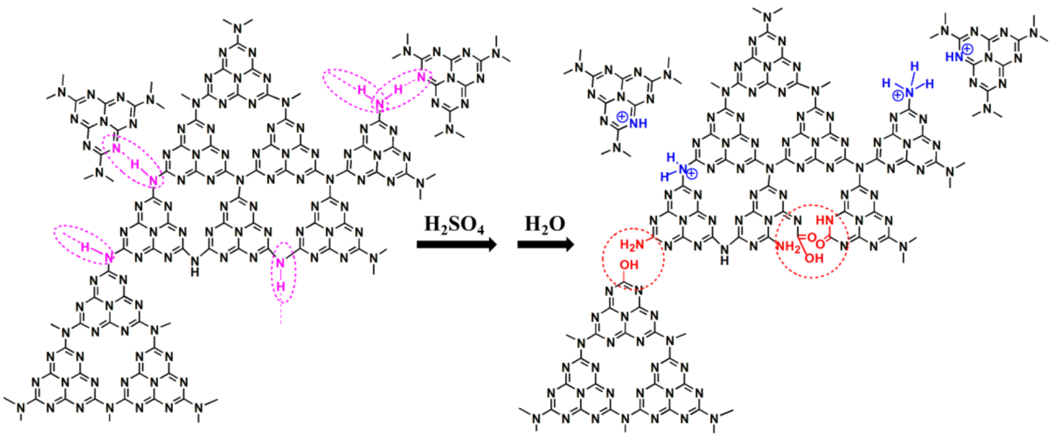

Fig. S8 Structure models of bulk g-C_3N_4 (left) and exfoliated g-C_3N_4 (right).

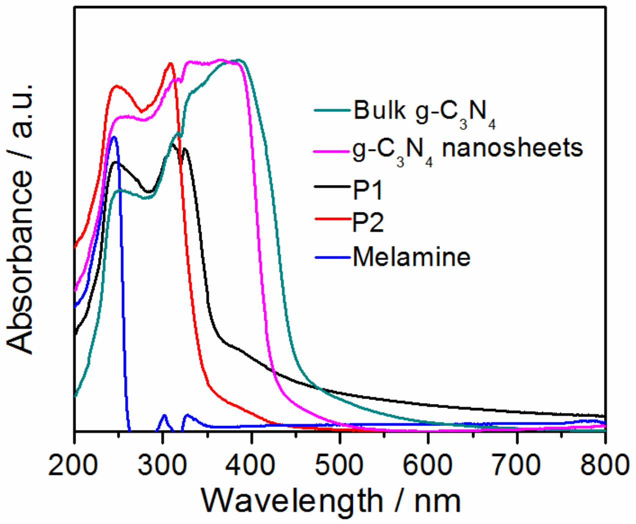

Fig. S9 UV-Vis DRS spectra of bulk g-C_3N_4, g-C_3N_4 nanosheets, P1, P2 and Melamine.

References

1 Y. G. Xu, H. Xu, L. Wang, J. Yan, H. M. Li, Y. H. Song, L. Y. Huang and G. B. Cai, *Dalton T*, 2013, **42**, 7604-7613.

2 Y. C. Zhao, D. L. Yu, H. W. Zhou, Y. J. Tian and O. Yanagisawa, *J Mater Sci*, 2005, **40**, 2645-2647.

3 B. V. Lotsch and W. Schnick, *Z Anorg Allg Chem*, 2006, **632**, 1457-1464.

4 V. W. H. Lau, M. B. Mesch, V. Duppel, V. Blum, J. Senker and B. V. Lotsch, *J Am Chem Soc*, 2015, **137**, 1064-1072.

5 L. Ming, H. Yue, L. Xu and F. Chen, *J Mater Chem A*, 2014, **2**, 19145-19149.